Experimental and Calculated Vibrational Spectra and Structure of Ziegler-Natta Catalyst Precursor: 50/1 Comilled $MgCl_2$-$TiCl_4$

Luigi Brambilla,[1] *Giuseppe Zerbi,**[1] *Stefano Nascetti,*[2] *Fabrizio Piemontesi,*[2] *Giampiero Morini*[2]

[1]Dipartimento di Materiali, Chimica e Ingegneria Chimica G. Natta del Politecnico di Milano, Piazza Leonardo da Vinci, 32 20133 Milano, Italy
[2]Basell Polyolefins, Centro Ricerche G. Natta, 44100 Ferrara, Italy

Summary: The vibrational Infrared and Raman Spectra of a $MgCl_2$-$TiCl_4$ Ziegler-Natta catalyst precursor with a 50/1 $MgCl_2/TiCl_4$ ratio have been recorded. The Raman spectrum of this catalyst precursor, in the range 50-500 cm^{-1}, shows clear scattering lines which can be assigned to the complex $MgCl_2$-$TiCl_4$, well separated from those of the initial species. Analogous, but less clear signals can be found in the infrared spectrum. Vibrational symmetry analysis and quantum chemical calculations of suitable models of $MgCl_2$-$TiCl_4$ complex have been made for the interpretation of the experimentally recorded spectra. The observed spectroscopic signals can be explained in terms of the existence of only one type of $MgCl_2$-$TiCl_4$ complex where the $TiCl_4$ molecules are complexed on the $MgCl_2$ along the (110) lateral cuts in a local C_{2v} symmetry with the Ti atoms in an octahedral coordination.

Keywords: infrared spectroscopy; quantum chemical calculations; Raman spectroscopy; $TiCl_4$; Ziegler-Natta catalyst

Introduction

$TiCl_4$ supported on activated $MgCl_2$ plays a fundamental role in the catalysis for the production of polyolefins[1]. On the basis of experimental evidence, suggesting that preferential lateral cuts corresponding to the (100) and (110) planes are formed during $MgCl_2$ activation[2], a variety of catalytic species have been proposed to occur when $TiCl_4$ is chemisorbed on coordinatively unsaturated Mg^{2+} ions located on the above side faces[3,4]. However, experimental evidence on the nature of the catalytic complexes are still lacking.

For the solution of this problem, several vibrational spectroscopic studies on Ziegler-Natta catalyst precursor have been reported[5-10]. Among these, most of the Infrared studies[5-8] have

 DOI: 10.1002/masy.200450926

been devoted to elucidate the nature of the complexes between the catalysts and the electron donors used in order to improve the stereospecificity in 1-olefin polymerization. Only Ystenes[9,10] reports that in the Infrared transmission spectra of $MgCl_2$-$TiCl_4$ precatalyst distinct bands near 450 cm^{-1} appear which can be assigned to the stretching of the terminal Ti-Cl bonds.
For the first time, the present study attempts to clarify the molecular structure of the $TiCl_4$ species complexed on $MgCl_2$ combining experimental Infrared and Raman vibrational spectroscopy data with quantum chemical calculations. In particular we focus our attention at one $MgCl_2$-$TiCl_4$ catalyst precursor, obtained by co-milling the two components in a 50/1 molar ratio.

Experimental

Pure $MgCl_2$ and $TiCl_4$ were purchased from Aldrich and used without further purification. $MgCl_2$, $TiCl_4$ and the catalyst precursor sample have been always handled and prepared in an inert atmosphere. The $MgCl_2$-$TiCl_4$ precatalyst with a 50/1 magnesium to titanium ratio was prepared by co-milling 12 g of $MgCl_2$ and 0.5 g of $TiCl_4$ in a 330 ml centrifugal mill containing 4 porcelain balls. The co-milling time was 4 hours. The Ti content in this catalyst precursor is comparable with that of some industrial catalysts for polyolefin polymerization[1].
Samples for Raman spectroscopy have been sealed in quartz tubes with a diameter of 5 mm; to record the Far Infrared spectra, the materials have been suspended in nujol and sandwiched between non additivated polyethylene sheets. Raman spectra were recorded with a "Modular XY" Dilor spectrometer in a backscattering geometry. The green laser line at 514,5 nm from an Ar+ laser of Spectra Physics, model 2030, was used. The laser power on the sample has been always less that 5 mw. The far infrared spectra have been recorded with a Nicolet Magna 760 with a solid substrate FAR IR (® Nicolet) beam splitter and equipped with a polyethylene window DTGS detector.

Calculations

Quantum chemical calculations have been carried out to predict the equilibrium geometry of $TiCl_4$-$MgCl_2$ complex models and to calculate their vibrational spectra. Normal modes frequencies as well as infrared and Raman intensities have been included in the calculations.
The spectroscopic observables have been calculated always by *ab initio* RHF/6-31g using Gamess[11] and Gaussian 98[12] programs. A full energy minimization calculation has been

adopted only for the free $TiCl_4$ molecule in the tetrahedral geometry. In the other cases a constrained geometry energy minimization has been used to simulate the $MgCl_2$ crystal or to predict the vibrational properties of the $TiCl_4$ molecules when the symmetry changes from T_d to C_{2v}. Since the values of the calculated normal mode frequencies and absolute vibrational infrared and Raman intensities have been shown to be basis set dependent, we use as a reliable structural tool only the qualitative trend and the qualitative intensity ratios.

Results and Discussion

Useful information derive from Raman spectra of the $MgCl_2$-$TiCl_4$ complexes because for this class of materials their Raman scattering lines are easy to be located and are well separated from those of isolated $TiCl_4$ or $MgCl_2$ species. On the contrary, the interpretation of the Far-Ir spectra is not so easy since the signals characteristic of the complex are weak if compared to the very strong vibrational transitions of $MgCl_2$ which dominate a large range of the Far Infrared frequencies.

In table 1 we report the experimental frequencies of the Raman scattering lines and Infrared absorption bands for the compounds studied.

Liquid $TiCl_4$

The experimental Raman spectrum of $TiCl_4$ at room temperature, reported in Figure 1a, shows the characteristic Raman lines at 500, 389, 139 and 122 cm^{-1}.

Table 1. Infrared and Raman experimental vibrational frequencies for $TiCl_4$, $MgCl_2$ and $MgCl_2$-$TiCl_4$ (50/1).

Compound	Observed vibrational frequencies in cm^{-1}	
$TiCl_4$	Raman	122 m, 139 m, 389 s, 500 vw
	Far-Infrared	500 s
$MgCl_2$	Raman	157 v , 243 vs
	Far-Infrared	273 vs, 363 w, 405 w
$MgCl_2$-$TiCl_4$ 50/1	Raman	84 vw, 125 w, 157 ** w, 175 vw, 243** s, 293 w, 389 * vw, 449 m, 464 m
	Far-Infrared	262 ** vs, 363 ** m, 405 ** m, 475 vw
Relative intensity: vs=very strong, s=strong, m=medium, w=weak, vw=very weak . Line assigned to: * free $TiCl_4$ or vibration of the complex ; ** bulk $MgCl_2$		

Figure 1b gives the calculated Raman spectrum for the free and isolated molecule of $TiCl_4$ in a tetrahedral geometry. For the $TiCl_4$ molecule belonging to the T_d symmetry point group the irreducible representation for its 9 vibrational normal modes and their spectroscopic activity is the following:

$\Gamma_{vib} = A_1$ (Raman pol.) + E (Raman dep.) + $2F_2$ (IR, Raman dep.)

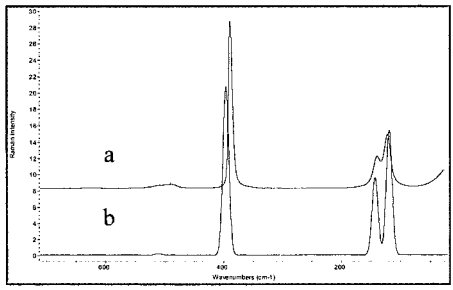

Figure 1. 1a) Experimental Raman spectrum of liquid $TiCl_4$ (λexc = 514.5 nm); 1b) ab initio calculated Raman spectrum of $TiCl_4$ in the tetrahedral structure.

For sake of simplicity we label the calculated vibrational frequencies as:

- ν_1, ν_2 and ν_3 the triply degenerate F_2 stretching mode of $TiCl_4$ at 511 cm^{-1} ;
- ν_4 the A_1 totally symmetric $TiCl_4$ stretching mode at 396 cm^{-1} ;
- ν_5, ν_6 and ν_7 the second triply degenerate F_2 mode at 143 cm^{-1};
- ν_8 and ν_9 the doubly degenerate E mode at 119 cm^{-1}.

The observed Raman signals are in full agreement with the predictions from group theory and the *ab initio* calculated spectra are in an exceptionally good agreement with the experiments.

The vibrational assignment then turns out to be straightforward and in agreement with those proposed previously in the literature[13,14].

Milled $MgCl_2$

Figure 2 reports the experimental infrared and Raman spectra of $MgCl_2$ milled for 8 hours, in the limited spectral range studied, with the characteristic sharp Raman lines at 157 and 243 cm^{-1} and the intense and broad infrared absorption bands at 273, 363 and 405 cm^{-1}.

Because all these vibrations are observed in the Raman and Far-Infrared spectra of the catalyst precursors we think that the bulk of the $MgCl_2$ is only slightly perturbed by the complexation process. Raman spectra are slightly influenced by the milling process while the Far-Infrared spectra show a general broadening of the vibrational bands with the increasing milling time logically connected with the electronic confinement due to the small size of the particles.

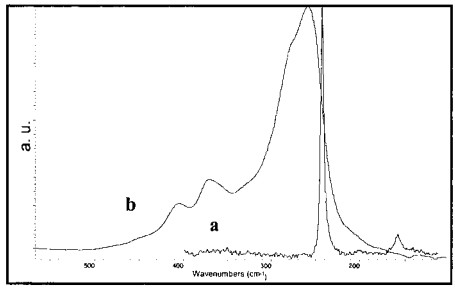

Figure 2. Experimental 2a) Raman spectrum (λexc = 514.5 nm) and 2b) Far-Infrared spectrum of 8 hours milled $MgCl_2$.

$MgCl_2$-$TiCl_4$ (50/1) catalyst precursor

The vibrational spectra of the 50/1 precursor have been considered; data on different mixtures will be reported elsewhere. In the Raman spectrum shown in Figure 3, in addition to the two lines at 243 and 157 cm^{-1}, ascribed to $MgCl_2$ and the very weak band at 389 cm^{-1} ascribed to free $TiCl_4$ or probably due to a vibration of the complex (see table I), the following lines are clearly observed: a broad Raman scattering centred near 464 cm^{-1} from which a stronger and sharp component appears at 449 cm^{-1}, a weak line at 293 cm^{-1}, very weak and hardly detectable lines near 84, 125 and probably at 175 cm^{-1}.

The Far IR spectrum (Figure 4) shows only a very weak and broad band centered near 475 cm^{-1} (expanded in the insert) floating on the wing of the strong absorption of $MgCl_2$. The observation of other IR transitions is made practically impossible by the strong and broad absorption of $MgCl_2$ which dominates the whole spectral range.

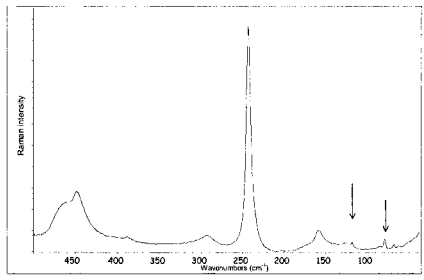

Figure 3. Raman spectrum (λexc = 514.5 nm) of $MgCl_2$-$TiCl_4$ (50/1) complex. The sharp and narrow peaks at low wavenumbers, indicated with arrows in Figure 4, are plasma laser lines.

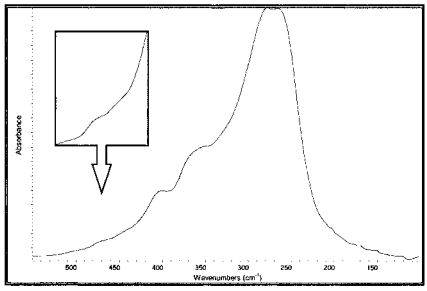

Figure 4. Far-Infrared spectrum of $MgCl_2$-$TiCl_4$ (50/1) complex.

The origin of the new vibrational transitions observed in the Raman and infrared spectra can be ascribed to the vibrational motions mostly localized on the $TiCl_4$ molecule which must have taken up another geometry as a consequence of the formation of the complex on the $MgCl_2$ surface.

It is generally accepted that lateral cuts corresponding to (110) and (100) $MgCl_2$ crystal planes are preferentially formed during precatalyst preparation[2] and different sites on activated $MgCl_2$ surface have been proposed for the $TiCl_4$ complexation[15-17]. When $TiCl_4$ molecules react with undercoordinated Mg^{2+} ions belonging to these two lateral cuts (tetracoordinated along the (110) and pentacoordinated along the (100)) can form complexes of different geometry.

For this reason many theoretical models[1] for the $TiCl_4$-$MgCl_2$ complexes have been proposed, both on (110) and (100) lateral cuts with the $TiCl_4$ molecules either in monomeric or dimeric

species[18]

In our theoretical analysis we have studied the spectroscopic properties of $TiCl_4$ molecules involved in the simplest and energetically most favoured complexes of the monomeric species proposed in literature[19]; in particular we have considered:

i) a geometry with $TiCl_4$ complexed along the $MgCl_2$ (110) lateral cut with the Ti atom in an octahedral coordination directly interacting with the $MgCl_2$, Figure 5a;

ii) a geometry with $TiCl_4$ complexed along the $MgCl_2$ (110) lateral cut with the Ti atom in a slightly distorted tetrahedral coordination interacting with $MgCl_2$ by two Cl atoms, Figure 5b;

iii) a geometry with $TiCl_4$ complexed along the $MgCl_2$ (100) lateral cut in a distorted trigonal bipyramid geometry, Figure 5c.

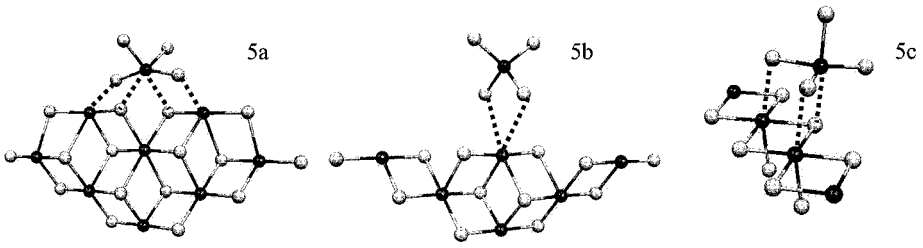

Figure 5. Models studied for the complexation of monomeric $TiCl_4$ on $MgCl_2$ crystal.

For case i) various authors[3,4] have proposed that upon complexation on the (110) lateral cut of $MgCl_2$,$TiCl_4$ tends to reach an octahedral coordination (Figure 5a). In such complex $TiCl_4$ takes up a local C_{2v} symmetry with the following spectroscopic activity:

$\Gamma_{vib} = 4A_1$ (IR, Raman) + A_2 (Raman) + $2B_1$ (IR, Raman) + $2B_2$ (IR, Raman)

We have followed the evolution of the vibrational spectra from the free molecule (T_d symmetry) to the molecule in the complex (C_{2v} symmetry) by carrying out several *ab initio* calculations of the vibrational spectra where one of the Cl-Ti-Cl valence angles is increased step-wise at a fixed value starting from the tetrahedral angle and reaching 180°. For each value of the angle energy minimization has been carried out and then in this constrained optimized geometry the vibrational spectra, infrared and Raman, have been calculated. The evolution of the calculated vibrational frequencies (vs. Cl-Ti-Cl valence bond angle) and their symmetry species are reported in Figure 6.

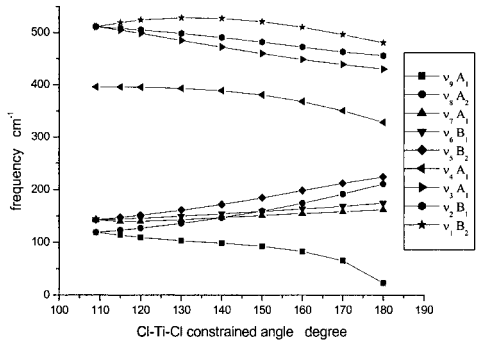

Figure 6. *Ab initio* calculated dispersion of the vibrational frequencies vs. Cl-Ti-Cl valence bond angle for $TiCl_4$ molecule from T_d to C_{2v} symmetry by stepwise opening of one Cl-Ti-Cl valence bond angle.

The symmetry properties of the normal modes of the starting tetrahedral $TiCl_4$ molecule are obvious when considering the structure of the irreducible representation and the degeneracy of the modes. Because of the lowering of the symmetry the F_2 mode near 511 cm^{-1} splits into a triplet ν_1, ν_2 and ν_3. The A_1 mode ν_4 obviously does not show splitting. The second F_2 mode splits in a triplet ν_5, ν_6 and ν_7, while the E mode splits in a doublet ν_8 and ν_9. It is obvious that the calculated changes of the normal vibrations ν_i , which are the solutions of the vibrational secular equation, describe the changes of the curvature of the vibrational potential

$$\left(\frac{\partial^2 V}{\partial Q_i^2}\right)_{eq.} \tag{1}$$

in the normal coordinate space at each equilibrium configuration, i.e.

$$2V = \sum_i \left(4\pi^2 c^2 \upsilon_i^2\right) Q_i^2 \tag{2}$$

This is precisely the additional information we derive from the vibrational spectra on the evolution of the electronic structure of $TiCl_4$ when approaching $MgCl_2$.

If it is assumed that the vibrational motions in the complex are still localized, such that the symmetry properties of C_{2v} point groups are satisfactorily maintained, it is worth looking at the repulsion of the vibrational levels which belong to the same symmetry species, as reported in Figure 6.

The calculated Raman spectra reported in Figure 7a show the increase in intensity of the ν_3 (A_1 component) of the F_2 vibration at 511 cm^{-1} with the parallel decrease in intensity of the ν_4 (A_1) vibration when the Cl-Ti-Cl bond opened. The calculated infrared spectra reported in Figure 7b show that when the Cl-Ti-Cl valence angle is opened the vibration at 511 cm^{-1} (IR strong) splits into a triplet with a redistribution of the intensities among the three components.

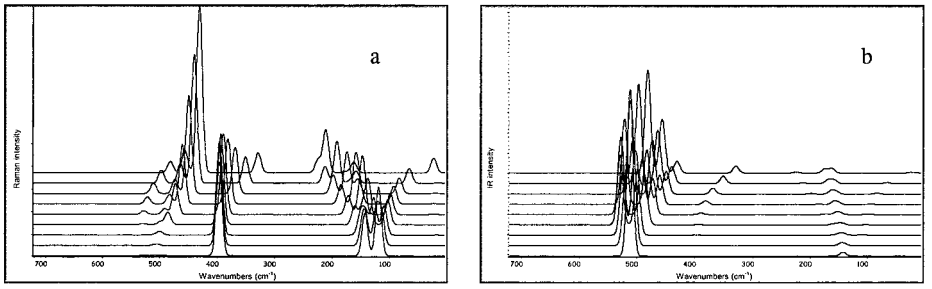

Figure 7. Evolution of *ab initio* calculated spectra for $TiCl_4$ molecule from T_d to C_{2v} symmetry by stepwise opening of one Cl-Ti-Cl valence bond angle: a) raman spectra and b) infrared spectra.

To take in account the influence of the $MgCl_2$ crystal on the vibrational properties of $TiCl_4$ we have carried out a calculation on the whole model 5a. The $TiCl_4$ molecule in a tetrahedral geometry was placed over the $MgCl_2$ crystal where the Cl and Mg atom have been keep fixed except the six atoms near the $TiCl_4$ molecule. After the constrained energy minimization the initial tetrahedral geometry of the $TiCl_4$ complexed with $MgCl_2$ was changed in a new C_{2v} symmetry, with the Ti atom in an octahedral coordination. The calculated Cl-Ti-Cl valence bond angle of the atoms interacting with the crystal was 159.73 degree.

The calculated Raman spectrum, in Figure 8a, shows a number of lines larger than that observed in Figure 7. Some of these bands, near 280, 310 and 3870 cm^{-1} (indicated with * in Figure 8a), do not seem to have any correspondence in the experimental spectra; this is obviously related to the fact that the model of $MgCl_2$ crystal considered in the calculations has finite dimensions. However a comparison of the calculated and experimental spectra in Figure 8b reveals the that vibrations mostly localized on the $TiCl_4$ molecule or due to collective motions of the $MgCl_2$ (indicated by arrows) are satisfactorily predicted.

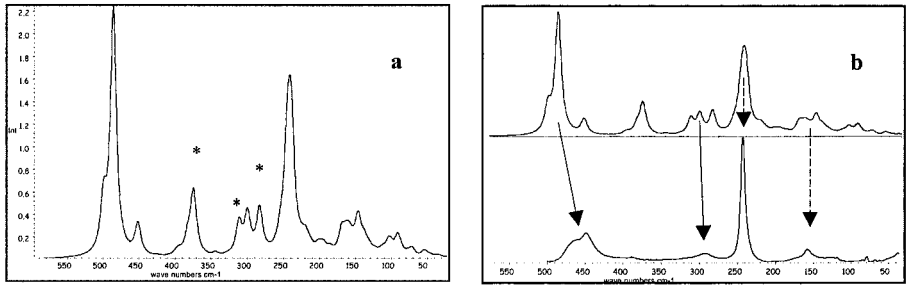

Figure 8. 8a) calculated Raman spectrum of model 5a; 8b) comparisons of 8a with the experimental Raman spectrum of $MgCl_2$-$TiCl_4$ 50/1. Solid arrows indicate vibrational transitions localized of $TiCl_4$, dashed on $MgCl_2$.

The role of the $MgCl_2$ lattice is an important issue in our work and has been carefully considered in this work. Several calculations have been carried out on a variety of models ranging from the free $TiCl_4$ which changes its geometry to various $TiCl_4$-$MgCl_2$ complexes where the number of $MgCl_2$ molecules in the chunks of lattice considered has been changed. Obviously an infinite perfect crystal of $MgCl_2$ could not be considered in the calculations; moreover because of milling the nanoparticles of $MgCl_2$ could show logical confinement effects, causing perturbations of its electron and phonons.

Calculations have shown that the forces between $TiCl_4$ and $MgCl_2$ lattice are not so strong to significantly perturb the dynamics of either the $TiCl_4$ molecule or the $MgCl_2$ cluster. The dynamical coupling of $TiCl_4$ in the complex is restricted on the surface of the $MgCl_2$, thus removing any worries about the size of the support made up by $MgCl_2$.

On the basis of the above calculations, it becomes possible to reach an interpretation of the experimental infrared and Raman spectra of the $MgCl_2$-$TiCl_4$ complex. Concerning the "isolated" $TiCl_4$ in a C_{2v} symmetry (Figure 7), for the triplet in the 400-500 cm^{-1} range, only two of the three components ν_1 and ν_2 are observed near 460 cm^{-1} in the infrared spectrum while the third component ν_3 at 449 cm^{-1} is observed in the Raman spectrum. This assignment is also supported by the fact that ν_3 is an A_1 mode (generally strong in the Raman) and must also be coupled with the other strong A_1 mode (ν_4) at 387 cm^{-1}, as clearly shown by the repulsion of the two levels

when the geometry is changed (Figure 6). Moreover the experimental Raman spectrum shows the right intensities redistribution between the A_1 vibrations (ν_3 and ν_4) predicted by the quantum chemical calculations.

Turn to the Raman spectrum of the complex 50/1 (Figure 8a, 8b) it shows practically the same features of TiCl4 in C2v symmetry as discussed before (Figure 7).

The experimental and theoretical results turn out undoubtedly to be in very good agreement and the reported evidence suggests that, when $TiCl_4$ is complexed on $MgCl_2$ at the 50/1 $MgCl_2/TiCl_4$ molar ratio, its geometry evolves from the initial tetrahedral structure to a new C_{2v} symmetry with the Ti approaching an octahedral coordination.

For case ii) the vibrational properties of a $TiCl_4$ molecule in a slightly distorted tetrahedral geometry have been considered, based on a $TiCl_4$ complexed on $MgCl_2$ along the (110) lateral cut with the Ti atom tetracoordinated[19] (Figure 5b). In such complex $TiCl_4$ takes up a local C_{2v} symmetry as in the previous case. Stepwise increases of the bond distance Ti-Cl of a pair of Ti-Cl bonds have been introduced in the calculations by constraining the Ti-Cl bond length from a $d_{Ti\text{-}Cl}$ = 2.202 Å to 2.43 Å. At every step the infrared and Raman spectra have been re-calculated after geometry re-optimization. Within this range of values for $d_{Ti\text{-}Cl}$, the Cl-Ti-Cl valence angles of $TiCl_4$ turn out to remain nearly tetrahedral.

The evolution of the calculated vibrational frequencies (vs. Cl-Ti-Cl valence bond length) and their symmetry species are reported in Figure 9. The calculated Raman and infrared spectra reported in Figures 10a and 10b show that:

- within the F_2 triplet near 551 cm^{-1} ν_1 shifts upward, ν_2 (A_1) stays almost unchanged while ν_3 shows a strong dispersion toward lower frequencies without an appreciable decrease of the infrared intensity;
- ν_2 (A_1) increases its Raman intensities only for large values of the Ti-Cl bond length;
- ν_4 (A_1) shifts substantially towards lower frequencies without any appreciable decrease of its Raman intensity and remains the strongest Raman line for any value of the Ti-Cl bond lengths considered;
- ν_5 to ν_9 keep their frequencies practically unchanged.

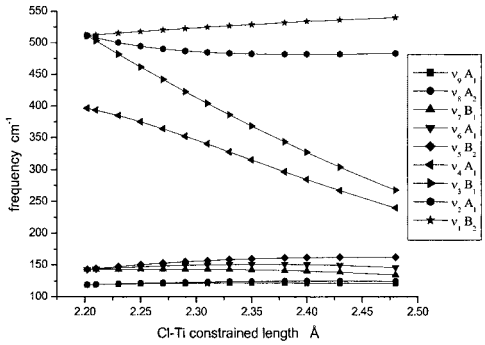

Figure 9. *Ab initio* calculated dispersion of the vibrational frequencies vs. Ti-Cl bonds lengths for $TiCl_4$ molecule by stepwise increasing of two Ti-Cl bonds from 2.202 Å (calculated length for the tetrahedral symmetry) to 2.48 Å.

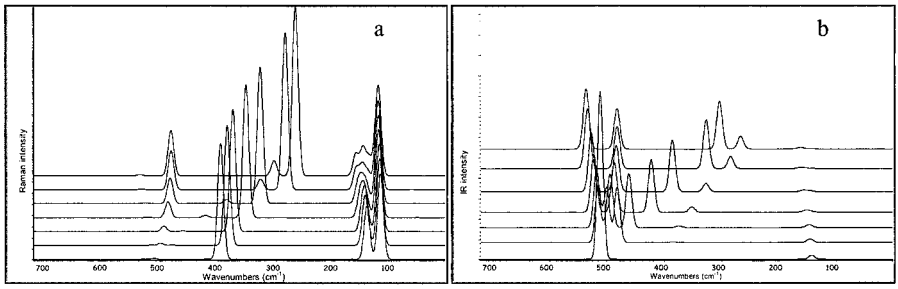

Figure 10. Evolution of: 10a) calculated Raman spectra and 10b) calculated infrared spectra of a $TiCl_4$ molecule from T_d to C_{2v} symmetry by stepwise increasing of two Ti-Cl bonds.

The calculated Raman spectrum of model 5b is reported in Figure 11a. Figure 11b reports the comparison between calculated and experimental spectra.

From the calculations it turns out that the complexed $TiCl_4$ molecule keeps substantially the tetrahedral geometry: the calculated Cl-Ti-Cl angle of the two Cl atoms interacting with the $MgCl_2$ has the values of 102.78 degree with a Ti-Cl bond length of 2.221 Å. This is reflected in the Raman spectrum where the vibrations localized on $TiCl_4$ molecule occur very close to those of the free $TiCl_4$.

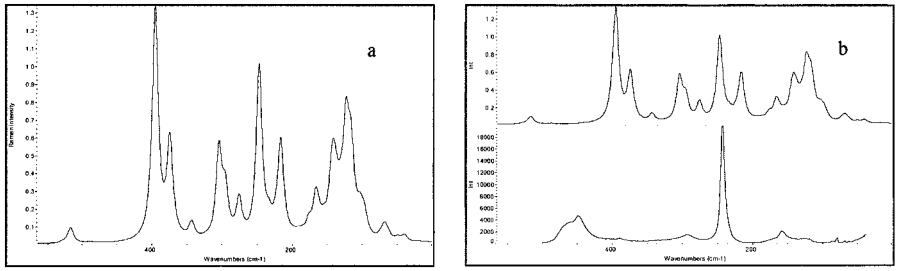

Figure 11. 11a) calculated Raman spectrum of model 5b; 11b) comparisons of 11a) with the experimental Raman spectrum of $MgCl_2$-$TiCl_4$ 50/1.

Evidence is gathered which shows that the experimental spectra of the $MgCl_2$-$TiCl_4$ (50/1) precursor do not show an acceptable agreement with the spectra of the model considered.

For the case iii) we have calculated only the infrared and Raman spectra of the molecule complexed on the (100) lateral cut, model 5c, because there is no unique way (contrary to the previous cases) to reach the desired geometry starting from the T_d structure of the free $TiCl_4$.

In such complex $TiCl_4$ takes up a local C_s symmetry with the following spectroscopic activity:

Γ_{vib} = 6A'(IR, Raman) + 3A"(IR, Raman)

The calculated infrared and Raman spectra are shown in Figure 12.

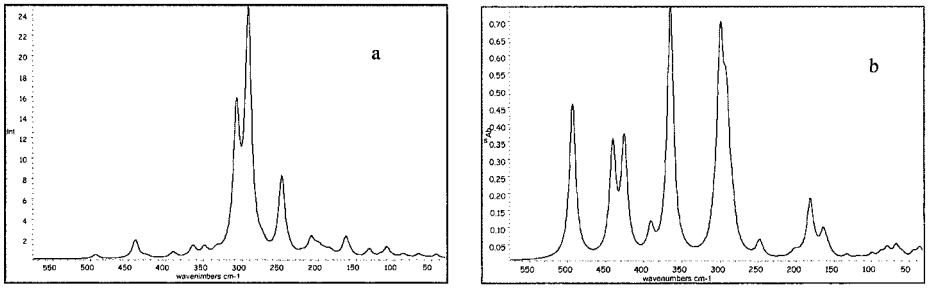

Figure 12. 12a) calculated Raman spectrum and 12b) calculated infrared spectrum of model 5c.

Band frequencies and intensities do not seem in a good agreement with the experimental results. As a result, only the structure of the $TiCl_4$ complex described in i) and represented in Figure 5a seems to be supported by the experimental vibrational spectra of the 50/1 complex.

Conclusions

In this paper we focused our attention on the structure of the complex $MgCl_2$-$TiCl_4$ in the 50/1catalyst precursor. Our conclusion is based both on the experimental results and on *ab initio* calculations.

The vibrational transitions observed in the Raman and infrared spectra can be ascribed to the vibrational motions mostly localized on the $TiCl_4$ molecule; it turns out that the vibrational motions of $TiCl_4$ are not strongly coupled with the modes of the $MgCl_2$ crystal.

At this low $TiCl_4$ concentrations (50/1) only one type of complex seems to occur on $MgCl_2$. The $TiCl_4$ molecule is forced to lower its symmetry from a full symmetrical T_d free species to almost an octahedral coordination of the Ti atom in the complex.

For the first time a clear indication of the octahedral geometry of $TiCl_4$ molecules absorbed on $MgCl_2$ is obtained from vibrational spectroscopy suggesting that the new species are bonded at the (110) lateral cut of $MgCl_2$ also in agreement with recent calculations [19].

The formation of octahedral $TiCl_4$ species on $MgCl_2$ on supported Ziegler Natta catalysts is usually accepted as model of aspecific catalytic sites in propylene polymerization (Corradini model, see ref. 3 and 20). Corradini indicated the monomeric titanium species on (110) lateral surface as possible aspecific sites producing the amorphous polymer.[20]

It is well known that $MgCl_2$-$TiCl_4$ catalysts are poorly isospecific in the polymerization of propylene as only about 40-50 % of isotactic polymer is obtained in the absence of Lewis bases acting either as internal or as external donor. Signals of different catalytic sites (possibly isospecific) may be expected, but the presence of a very low amount of titanium in our model system may not give enough Raman intensity to make them detectable.

The influence of the amount of titanium bonded on $MgCl_2$ on both infrared and Raman spectra and on the performance of the corresponding Ziegler-Natta catalysts in propylene polymerization is under evaluation and it will be presented in a future work.

Acknowledgement

Antonio Cristofori and Antonella Coraini are gratefully acknowledged for sample preparation, Leonardo Contado for the recording of the far infrared spectra and Matteo Tommasini for the calculated Raman spectra.

In the early stages of this work we have enjoyed the competent and thoughtful discussions with the late Professor Ugo Giannini we all miss.

[1] E. Albizzati, U. Giannini, G. Collina, L. Noristi, L. Resconi, in: "*Polypropylene Handbook*", Moore E.P. Jr., Eds., Carl Hanser Verlag, Munich **1996**, p. 11.
[2] U. Giannini, G. Giunchi, E. Albizzati, P.C. Barbè, in: "*Recent Advances in Mechanistic and Synthetic Aspects of Polymerization*", NATO ASI Sect. 215, Fontanille, M., Guyot, A., Eds., Reidel **1987**, p. 473.
[3] P. Corradini, V. Busico, G. Guerra, in: "*Comprehesive Polymer Science*", G.C. Eastmann, A. Ledwith, S. Russo, P. Sigwalt, Eds., Pergamon, **1989**, Vol. *4*, p. 29.
[4] L. Barino, R. Scordamaglia, *Macromol. Chem. Theory Simul.* **1998**, *7*, 407.
[5] E. Ritter, Ø. Nirisen, S. Kvisle, M. Ystenes, H.A. Øye, *in "Transition Metal Catalyzed Polymerizations*", R.P. Quirk Eds., Cambridge University Press, Cambridge **1988**, p. 292.
[6] M. Terano, T. Kataoka, T. J. Keii, *Polym.* Sci., Part A: Polym. Chem. **1990**, *28*, 2035.
[7] R. Spitz, J.L. Lacombe, A. J. Guyot, *Polym. Sci., Part A: Polym. Chem.* **1984**, *22*, 264.
[8] J.C.W. Chien, J.C. Wu, C.I.J. Kuo, *Polym. Sci., Part A: Polym. Chem.* **1983**, *21*, 725.
[9] Ø. Bache, M.Ystenes, *Appl. Spectrosc.* **1994**, *48*, 985.
[10] Ø. Bache, M. Ystenes, Intern. *Symposium on Metallorganic Catalysts for Synthesis and Polymerization*, September 13, Hamburg **1998**.
[11] M.W. Schmidt, K.K. Baldridge, J.A. Boatz, S.T. Elbert, M.S. Gordon, J.H. Jensen, S. Koseki, N. Matsunaga, K.A. Nguyen, S. Su, T.L. Windus, M. Dupuis, J.A. Jr Mongomery, *J. Comput. Chem.* **1993**, *14*, 1347.
[12] M.J. Frisch, G.W. Trucks, H.B. Schlegel, G.E. Scuseria, M.A. Robb, J.R. Cheeseman, V.G. Zakrzewski, J.A. Montgomery, R.E. Stratmann, J.C. Burant, S. Dapprich, J.M. Millam, A.D. Daniels, K.N. Kudin, M.C. Strain, O. Farkas, J. Tomasi, V. Barone, M. Cossi, R. Cammi, B. Mennucci, C. Pomelli, C. Adamo, S. Clifford, J. Ochterski, G.A. Petersson, P.Y. Ayala, Q. Cui, K. Morokuma, D.K. Malick, A.D. Rabuck, K. Raghavachari, J.B. Foresman, J. Cioslowski, J.V. Ortiz, B.B. Stefanov, G. Liu, A. Liashenko, P. Piskorz, I. Komaromi, R. Gomperts, R.L. Martin, D.J. Fox, T. Keith, M.A. Al-Laham, C.Y. Peng, A. Nanayakkara, C. Gonzalez, M. Challacombe, P.M.W. Gill, B.G. Johnson, W. Chen, M.W. Wong, J.L. Andres, M. Head-Gordon, E.S. Replogle, J.A. Pople, *Gaussian 98, Revision A.7*, Gaussian Inc., Pittsburgh, PA, **1998**.
[13] K. Nakamoto, in "*Infrared and Raman spectra of inorganic and coordination compounds*", Wiley, New York **1997**.
[14] R. J. H. Clark, *J. Chem. Soc (A)*, **1971**, 2999.
[15] E. Puakka, T. T. Pakkanen, T. A. Pakkanen, *Surf. Sci.* **1995**, *334*, 289.
[16] U. Giannini, *Makromol. Chem. Suppol.* **1981**, *4*, 216.
[17] P. Corradini, V. Barone, R. Fusco, G. Guerra, *Gazz. Chim. Ital.* **1983**, *113*, 601.
[18] A. G. Potapov, V. V. Kriventsov, D. I. Kochubey, G. D. Bukatov, V. A. Zakharov, *Macromol. Chem. Phys.* **1997**, *198*, 3477.
[19] G. Monaco, M. Toto, G. Guerra, P. Corradini, L. Cavallo, *Macromolecules* **2000**, *33*, 8953.
[20] P. Corradini, V. Barone, R. Fusco, Gazzetta Chimica Italiana **1983**, *113*, 601.